Manuscript refereed by Prof Ilaria Cristofolini (University of Trento, Italy)

Maximum in Mass Flow Rates of Hard Metal Granules through Circular Orifices in Relation to the Angle of Repose

Marvin Just[1,2] marvin.just@ceratizit.com, Alexander Medina Peschiutta[1,2] alexander.medina@uni.lu, Ralph Useldinger[1] ralph.useldinger@ceratizit.com, Jörg Baller[2] joerg.baller@uni.lu

[1]CERATIZIT Luxembourg S.à r.l., 101 Route de Holzem, L-8232, Grand Duchy of Luxembourg
[2]Department of Physics and Materials Science, University of Luxembourg, 162A Avenue de la Faiencerie, L-1511 Luxembourg, Grand Duchy of Luxembourg

Abstract

The mass flow of granular matter through orifices can be described by the well-known Beverloo law. It depends on particle and orifice sizes, interparticle and particle/container interaction forces, particles' surfaces - to name a few influences on the mass flow rate. We present an experimental study of the flow of a set of ready-to-press (RTP) hard metal powders through orifices of varying diameter. The obtained parameters of the Beverloo law are compared with angle of repose measurements. The interplay between attractive interparticle forces and gravitational forces are discussed for both types of experimental measurements and related to the difference between particle and orifice size.

Introduction

The flowability of granular materials is essential for filling applications, e.g. the filling step within a compressing cycle or for powder based additive manufacturing processes [1]. The flowability of granular and powder-like materials can be expressed by the mass flow rate, measured, for instance, with a Hall flow meter, as described in ASTM B213 [2]. The mass flow rate strongly depends on the experimental setup, such as inner hopper angle [3], hopper design [4], orifice size [5], and on the properties of the granular materials, e.g. size distribution [6,7] and particle shape [8]. A better understanding of these influences is challenging yet essential to manufacture bulk materials with defined properties.

Beverloo et al. [9] investigated the mass flow rate of various coarse-grained materials through a circular orifice and a cylindrical tube. Based on the findings and the properties of the materials, a model was proposed, the so-called Beverloo Law, to predict the mass flow rate as follows:

$$\dot{m} = C\rho_b\sqrt{g}\sqrt{(D-kd)^5} \quad (1)$$

Where ρ_b is the bulk density, g is the gravitational acceleration, D is the orifice diameter, and d is the particle diameter of the granular system. C and k are dimensionless fitting parameters ranging from 0.55 to 0.65 and 1 to 3 [9], respectively. Furthermore, the experimental study of Beverloo et al. [9] state that flows in a zone near the orifice perimeter alters the flow through the orifice, minimising the orifice diameter D to an effective diameter D_{eff}, which scales with the material's particle diameter d (Equation 2).

$$D_{eff} = D - kd \quad (2)$$

The parameters C and k must be determined experimentally for each powder system. Many researchers are interested in understanding the meaning of the fitting parameters C and k to improve the empirical model (Equation 1) and to predict the mass flow rate. Literature does not show a unique picture of the link between the fitting parameters and material properties or experimental conditions. C is e.g. shown to depend on the hopper geometry [10] and of powder properties such as the friction coefficient [11]. The fitting parameter k is influenced by powder properties such attraction forces between particles [12] and particle shape [13,14].

The objective of this experimental study is to contribute to the understanding of the influences on the parameters C and k for one class of materials: hard metal granules. This is realized by measuring the mass flow rate with a cylindrical tube and flat-bottomed orifices for a set of hard metal granular systems with

 https://doi.org/10.59499/EP235765170

varying particle size distribution. The fitting parameters C and k are determined from the acquired mass flow rates, and they are compared to the friction coefficient (from angle of repose measurements) and to interparticle forces expressed by the granular Bond number.

Experimental methods

Materials

For this experimental study, a hard metal granule grade containing 9 wt.% of cobalt has been manufactured via a spray drying process at CERATIZIT Luxembourg S.à r.l.. The granular material is sieved, using various sieving meshes, to acquire granular systems with specific granular size distributions. Subsequently, the granular size distribution is determined using a laser diffraction particle size analyzer (Mastersizer 3000 from Malvern), and the volume-to-surface mean diameter, represented by the Sauter mean diameter $d_{[3,2]}$, is calculated. The physical meaning of the Sauter mean diameter can be found in reference [15].

The bulk and tapped density of the sieved and unsieved samples are measured with the device Granupack from Granutools. The device measures the density under the continuous movement of a cylinder, introducing kinetic energy into the system and enabling a rearrangement of the granules. The axial movement per tap is 1 mm. The material is tapped for 100 taps at a frequency of 1 s^{-1}, changing beyond 100 taps to 2 s^{-1} until the maximum tap number of 500. The first measurement point (tap number = 0) corresponds to the bulk density, whereas the final density (tap number = 500) describes the tap density. The pycnometer density is measured with the pycnometer Accupyc II 1340 from Micromeritics using helium as measurement gas.

The mass flow rate $\dot{m}$ is measured with the flowmeter Granuflow from Granutools. The device consists of a metallic cylinder placed on a metallic disc. For the measurements presented in this study, 600 g of sample material is poured into the cylindric container. The metallic disc has several circular orifices with diameters D of 1, 2, 3, 4, 5, 6 and 8 mm from which the granular material falls onto a balance.

A novel approach described in detail in [16] is employed to measure the angle of repose. The measurement device comprises a funnel with a 2 mm orifice and a movable plate below the funnel. The granules fall onto the plate, and a camera captures the evolution of the bulking and avalanching phases. The resulting images are processed to calculate the angle of repose.

Results and Discussion

Characterization of the materials

Table 1 displays the characteristics of the granular materials investigated.The samples differ in the mean particle diameter and the width of the particles size distribution (in µm): narrow (63-100, 100-125, 125-150, 150-200, 200-224), medium (125-200, 150-224), broad (125-224) and the extremes (>224, <125). All samples have been produced from the same mother batch (unsieved).

The cohesive behaviour of a granular material can be quantified using the granular Bond number which represents the interplay between the main forces acting on the particles: attractive interaction on one hand and gravitational force on the other hand. Table 1 presents the granular Bond number based on the experimental study of Just et al. [17], where atomic force microscopy (AFM) was utilised to measure the attractive forces between particles of the same material class as in this study.

 https://doi.org/10.59499/EP235765170

Table 1: Granular characteristics of sieved samples, values from [16] *and completed with information from* [17].

Sieving Class	Sauter diameter $d_{[3,2]}$ (µm)	Bulk density ρ_b (g/cm^3)	Tap density ρ_{tap} (g/cm^3)	Pyc. density ρ_{pyc} (g/cm^3)	Granular Bond number Bo_g (-), 100% Error
Unsieved	159 ± 4	3.36 ± 0.01	3.66 ± 0.01	11.50 ± 0.01	0.04
>224	241 ± 2	3.26 ± 0.01	3.51 ± 0.01	11.50 ± 0.01	0.02
200-224	212 ± 1	3.27 ± 0.01	3.51 ± 0.01	11.52 ± 0.01	0.02
150-224	177 ± 3	3.27 ± 0.01	3.52 ± 0.01	11.52 ± 0.01	0.03
150-200	170 ± 1	3.28 ± 0.01	3.53 ± 0.01	11.52 ± 0.01	0.03
125-224	165 ± 3	3.29 ± 0.01	3.55 ± 0.01	11.51 ± 0.01	0.03
125-200	161 ± 1	3.30 ± 0.01	3.56 ± 0.01	11.51 ± 0.01	0.03
125-150	127 ± 1	3.28 ± 0.01	3.54 ± 0.01	11.52 ± 0.01	0.06
100-125	104 ± 1	3.29 ± 0.01	3.55 ± 0.01	11.52 ± 0.01	0.08
63-100	79 ± 1	3.30 ± 0.01	3.58 ± 0.01	11.52 ± 0.01	0.14
<125	54 ± 1	3.37 ± 0.01	3.66 ± 0.01	11.53 ± 0.01	0.30

Impact of the attractive forces on the mass flow rate

Measurements of the mass flow rate $\dot{m}$ with various orifice diameters D are displayed in Figure 1 to Figure 3. For all measured mass flow rates, identical trends can be observed with increasing orifice diameters: As the granular Bond number increases, the mass flow rate also increases (circles). This effect is mainly caused by the decrease in the particle mean diameter (Equation 1). As the granular Bond number continues to increase, a decreasing mass flow rate can be observed (triangles), caused by the rising dominance of attractive interparticle forces.

Power law fits are applied to both regions in the mass flow rate curves in **Figure *1*** to **Figure *3***. The unsieved sample is neglected for both fits since the granular Bond number is only poorly defined for a material with such a broad distribution of particle sizes. The power law fits intersect at the maximal mass flow rate $\dot{m}_{max}$ for a given orifice size D and granular system. Noteworthy, the maximal flow rate $\dot{m}_{max}$ appears at a similar granular Bond number (between 0.05 and 0.07) independent of the orifice size D (**Figure *1*** to **Figure *3***) whereas the mass flow rates increase understandably with increasing orifice size D.

 https://doi.org/10.59499/EP235765170

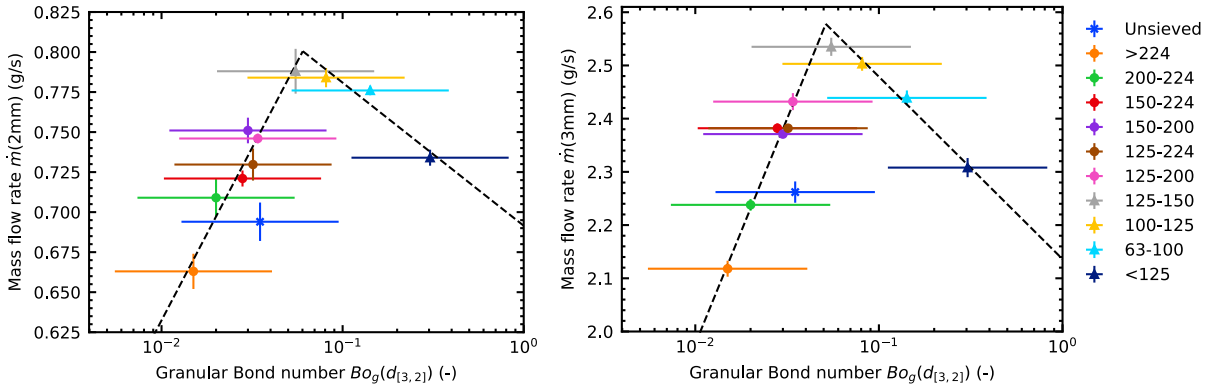

Figure 1. Mass flow rate in the function of the granular Bond number for orifice diameters 2 mm (left) and 3 mm (right). Both graphs share the same legend.

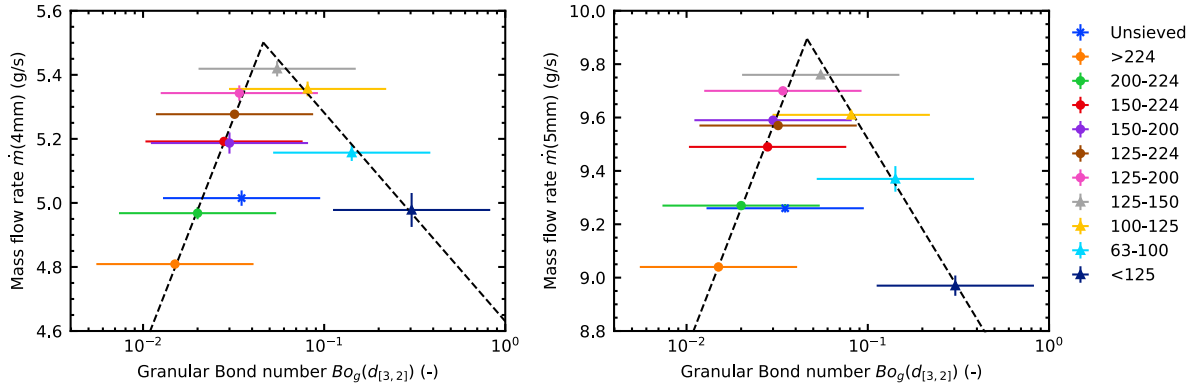

Figure 2. Mass flow rate in the function of the granular Bond number for orifice diameter 4 mm (left). Mass flow rates for an orifice of 5 mm (right) are from [17]. Both graphs share the same legend.

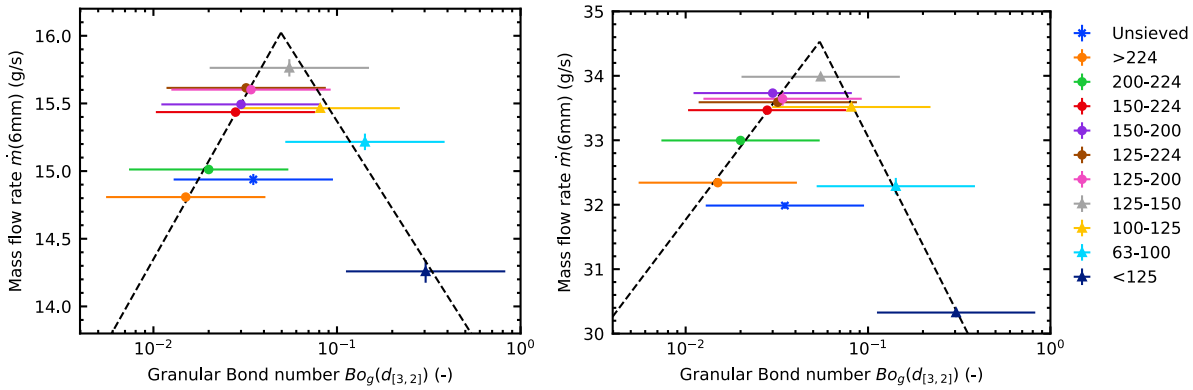

Figure 3. Mass flow rate in the function of the granular Bond number for orifice diameters 6 mm (left) and 8 mm (right). Both graphs share the same legend.

The impact of the friction coefficient and granular Bond number on the mass flow rate

Figure *4* (left) shows all the mass flow rates from **Figure *1*** to **Figure *3*** in one graph. The first step to determine the fitting parameters C and k is to plot the mass flow rate $\dot{m}^{0.4}$ in function of the orifice diameter D (**Figure *4***, right). Next, a linear fit for each measured sample is applied. Finally, the fitting parameters C and k can be derived from the slope and intercept, respectively. The intercept with the abscissa describes

 https://doi.org/10.59499/EP235765170

the minimal orifice diameter $D_0(\dot{m} = 0$ g/s), which can be used to determine the fitting parameter k considering the granular mean diameter ($D_0/d = k$) from Table 1.

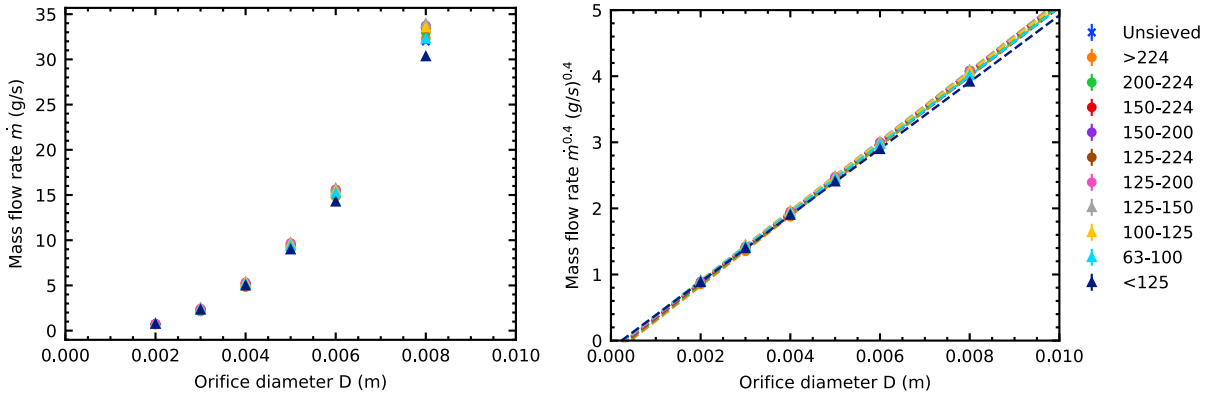

Figure 4. Mass flow rate in the function of the orifice diameter D (left) and the linear relationship of the mass flow rate $\dot{m}^{0.4}$ in the function of the orifice diameter D to determine the fitting parameter C and k (right). Error bars are smaller than the marker size.

It is known that the particle-particle friction affects the fitting parameter C [11]. **Figure *6*** shows the fitting parameter C in function of the friction coefficient μ calculated from angle of repose measurements (μ = tan(α), where α is the angle of repose) [17]. It can be seen from the graph that the fitting parameters C varies between 0.5 and 0.65, being in the common range provided in literature for measurements with flat-bottomed orifices [9,10,18]. It decreases with increasing friction coefficient. This outcome appears intuitive as a higher friction coefficient also implies a higher resistance to flow, visible by a decrease in C. This observation has also been shown in a numerical study [11].

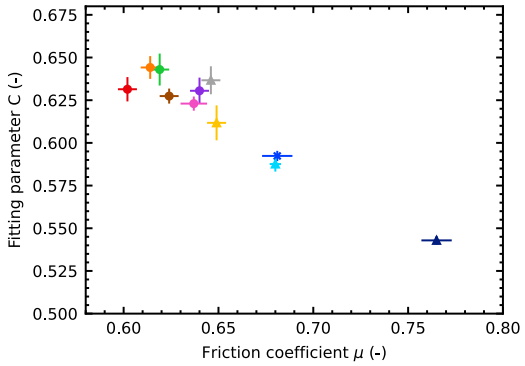

Figure 5. Fitting parameter C in function of the friction coefficient μ. The friction coefficients are acquired from [17]. Shared legend with Figure 6.

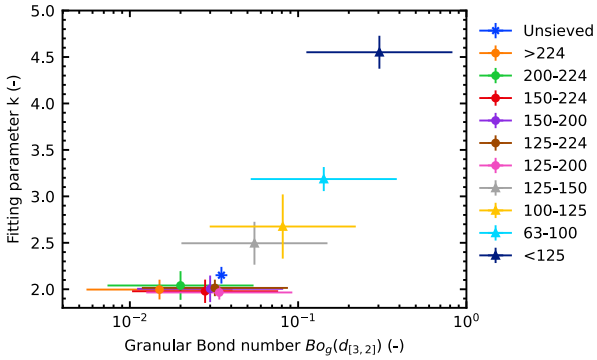

Figure 6. Fitting parameter k in dependency of the granular Bond number Bo_g.

Figure *6* displays the fitting parameter k as a function of the granular Bond number for the samples from Table 1. When the material is discharging through an orifice, which is larger than the minimal orifice diameter ($D>D_0$), the fitting parameter k reduces the orifice diameter D to an effective orifice diameter D_{eff} (Equation 2). This reduction is caused by increasing interparticle forces (with respect to the 'driving' gravitational forces). Two regions are present in **Figure *6***. In the first region, the fitting parameter k is nearly constant ($k \approx 2$) which means that for these small Bond numbers (which correspond to bigger particle sizes), particle-particle interactions do not play a role. Above Bond numbers of 0.05, the effective diameter D_{eff} is reduced by the interactions leading to increased values of the parameter k.

 https://doi.org/10.59499/EP235765170

Conclusion

In this study, we present mass flow rate measurements of a set of hard metal granules. The interplay between attractive interparticle forces and driving gravitational forces leads to a maximum of the mass flow rates which can be always found at the same granular Bond number – independent of the orifice size chosen for the experiments. The parameter C in the Beverloo law is found to be related to the friction coefficient which – in this study – is only changed by varying the particle diameters. The parameter k in the Beverloo law describes a reduction of the orifice diameter to an effective orifice diameter. The experiments show that this reduction is only relevant for granules with smaller diameters (higher granular Bond numbers) where interparticle forces become more dominant over gravitational forces. For the investigated hard metal granules, the maximum mass flow rate was found for particle diameters between 127 and 138 µm, but it is expected that this quantity depends also on other properties like e.g., tungsten carbide grain size. These findings are valuable in optimizing the mass flow rate in hard metal granular systems and can aid in the design and engineering of such systems.

Acknowledgements

This work was funded in whole, or in part, by the Luxembourg National Research Fund and by CERATIZIT Luxembourg S.à r.l. with two Industrial Fellowships grants. Grant acronyms and references are MEPFLOW [13320318] and RHAMEP [14187658].

References

[1] I. Baesso, D. Karl, A. Spitzer, A. Gurlo, J. Günster, A. Zocca, Characterization of powder flow behavior for additive manufacturing, Addit. Manuf. 47 (2021) 102250. https://doi.org/10.1016/j.addma.2021.102250.

[2] ASTM International, ASTM B213-13: Standard Test Methods for Flow Rate of Metal Powders using the Hall Flowmeter Funnel, ASTM Int. (2013). https://doi.org/10.1520/B0213-13.

[3] S. Albaraki, S.J. Antony, How does internal angle of hoppers affect granular flow? Experimental studies using digital particle image velocimetry, Powder Technol. 268 (2014) 253–260. https://doi.org/10.1016/j.powtec.2014.08.027.

[4] D. Sun, H. Lu, J. Cao, Y. Wu, X. Guo, X. Gong, Flow mechanisms and solid flow rate prediction of powders discharged from hoppers with an insert, Powder Technol. 367 (2020) 277–284. https://doi.org/10.1016/j.powtec.2020.03.053.

[5] J. Khanam, A. Nanda, Flow of granules through cylindrical hopper, Powder Technol. 150 (2005) 30–35. https://doi.org/10.1016/j.powtec.2004.11.016.

[6] J. Wu, J. Binbo, J. Chen, Y. Yang, Multi-scale study of particle flow in silos, Adv. Powder Technol. 20 (2009) 62–73. https://doi.org/10.1016/j.apt.2008.02.003.

[7] R. Kumar, S.R. Gopireddy, A.K. Jana, C.M. Patel, Study of the discharge behavior of Rosin-Rammler particle-size distributions from hopper by discrete element method: A systematic analysis of mass flow rate, segregation and velocity profiles, Powder Technol. 360 (2020) 818–834. https://doi.org/10.1016/j.powtec.2019.09.044.

[8] B. Sukumaran, A.K. Ashmawy, Influence of inherent particle characteristics on hopper flow rate, Powder Technol. 138 (2003) 46–50. https://doi.org/10.1016/j.powtec.2003.08.039.

[9] W.A. Beverloo, H.A. Leniger, J. van de Velde, The flow of granular solids through orifices, Chem. Eng. Sci. 15 (1961) 260–269. https://doi.org/10.1016/0009-2509(61)85030-6.

[10] R.O. Uñac, A.M. Vidales, O.A. Benegas, I. Ippolito, Experimental study of discharge rate fluctuations in a silo with different hopper geometries, Powder Technol. 225 (2012) 214–220. https://doi.org/10.1016/j.powtec.2012.04.013.

[11] T. Li, H. Zhang, M. Liu, Z. Huang, H. Bo, Y. Dong, DEM study of granular discharge rate through a vertical pipe with a bend outlet in small absorber sphere system, Nucl. Eng. Des. 314 (2017) 1–10. https://doi.org/10.1016/j.nucengdes.2017.01.008.

[12] A. Anand, J.S. Curtis, C.R. Wassgren, B.C. Hancock, W.R. Ketterhagen, Predicting discharge dynamics of wet cohesive particles from a rectangular hopper using the discrete element method (DEM), Chem. Eng. Sci. 64 (2009) 5268–5275. https://doi.org/10.1016/j.ces.2009.09.001.

[13] J. Tierrie, H. Baaj, P. Darmedru, Modeling the relationship between the shape and flowing

 https://doi.org/10.59499/EP235765170

characteristics of processed sands, Constr. Build. Mater. 104 (2016) 235–246. https://doi.org/10.1016/j.conbuildmat.2015.11.046.

[14] S.D. Liu, Z.Y. Zhou, R.P. Zou, D. Pinson, A.B. Yu, Flow characteristics and discharge rate of ellipsoidal particles in a flat bottom hopper, Powder Technol. 253 (2014) 70–79. https://doi.org/10.1016/j.powtec.2013.11.001.

[15] P.B. Kowalczuk, J. Drzymala, Physical meaning of the sauter mean diameter of spherical particulate matter, Part. Sci. Technol. 34 (2016) 645–647. https://doi.org/10.1080/02726351.2015.1099582.

[16] M. Just, A. Medina Peschiutta, F. Hippe, R. Useldinger, J. Baller, Determination of the angle of repose of hard metal granules, Powder Technol. 407 (2022) 117695. https://doi.org/10.1016/j.powtec.2022.117695.

[17] M. Just, A. Medina Peschiutta, F. Hippe, R. Useldinger, J. Baller, Gravitational mass flow measurements of various granular materials in relation to an extended Bond number, Int. J. Refract. Met. Hard Mater. 112 (2023) 106142. https://doi.org/10.1016/j.ijrmhm.2023.106142.

[18] Z. Zatloukal, Z. Šklubalová, Drained angle of free-flowable powders, Part. Sci. Technol. 26 (2008) 595–607. https://doi.org/10.1080/02726350802501369.

 https://doi.org/10.59499/EP235765170